A Critical Role of Lyst-Interacting Protein5, a Positive Regulator of Multivesicular Body Biogenesis, in Plant Responses to Heat and Salt Stresses[1]

Fei Wang, Yan Yang, Zhe Wang, Jie Zhou, Baofang Fan, and Zhixiang Chen*

Department of Botany and Plant Pathology, Purdue University, West Lafayette, Indiana 47907–2054 (F.W., Z.W., J.Z., B.F., Z.C.); and Department of Horticulture, Zijingang Campus, Zhejiang University, Hangzhou 310058, China (Y.Y., J.Z., Z.C.)

ORCID ID: 0000-0002-5472-4560 (Z.C.).

Multivesicular bodies (MVBs) are unique endosomes containing vesicles in the lumen and play critical roles in many cellular processes. We have recently shown that Arabidopsis (*Arabidopsis thaliana*) Lyst-Interacting Protein5 (LIP5), a positive regulator of the Suppressor of K^+ Transport Growth Defect1 (SKD1) AAA ATPase in MVB biogenesis, is a critical target of the mitogen-activated protein kinases MPK3 and MPK6 and plays an important role in the plant immune system. In this study, we report that the LIP5-regulated MVB pathway also plays a critical role in plant responses to abiotic stresses. Disruption of *LIP5* causes compromised tolerance to both heat and salt stresses. The critical role of LIP5 in plant tolerance to abiotic stresses is dependent on its ability to interact with Suppressor of K^+ Transport Growth Defect1. When compared with wild-type plants, *lip5* mutants accumulate increased levels of ubiquitinated protein aggregates and NaCl under heat and salt stresses, respectively. Further analysis using fluorescent dye and MVB markers reveals that abiotic stress increases the formation of endocytic vesicles and MVBs in a largely LIP5-dependent manner. LIP5 is also required for the salt-induced increase of intracellular reactive oxygen species, which have been implicated in signaling of salt stress responses. Basal levels of LIP5 phosphorylation by MPKs and the stability of LIP5 are elevated by salt stress, and mutation of MPK phosphorylation sites in LIP5 reduces the stability and compromises the ability to complement the *lip5* salt-sensitive mutant phenotype. These results collectively indicate that the MVB pathway is positively regulated by pathogen/stress-responsive MPK3/6 through LIP5 phosphorylation and plays a critical role in broad plant responses to biotic and abiotic stresses.

Multivesicular bodies (MVBs) are a subset of late endosomes that contain intraluminal vesicles generated when the limiting membrane of the endosome invaginates and buds into its own lumen. MVBs perform a variety of functions and, as a result, can have different compositions and morphologies. The most well-established role of MVBs in all eukaryotic cells is as a degradation route in the endocytic pathway that allows protein-containing intraluminal vesicles to be delivered into and degraded upon fusion with lysosomes or vacuoles (Reyes et al., 2011; Contento and Bassham, 2012). The route acts as a mechanism for removing damaged proteins as well as proteins that require down-regulation or clearing from the plasma membrane as part of a regulatory process. Those proteins retained in the limiting membrane of MVBs, on the other hand, can be delivered to the membrane of lysosomes or vacuoles or sorted back to the plasma membrane or other cellular compartments (Reyes et al., 2011; Contento and Bassham, 2012).

The protein machinery involved in MVB biogenesis has been well studied in yeast and other eukaryotic organisms. A majority of proteins required for protein sorting into MVBs are components of three distinct protein complexes named ESCRT-I, ESCRT-II, and ESCRT-III (for Endosomal Sorting Complexes Required for Transport; Winter and Hauser, 2006). These complexes are recruited to endosomal membranes and function in sorting cargo and the formation of intraluminal vesicles. Ubiquitinated membrane proteins are first recognized by specific ubiquitin-binding proteins that also recruit ESCRT-I components from the cytoplasm. ESCRT-II and ESCRT-III complexes are then recruited and transiently assembled on the endosomal membrane for cargo sorting, concentration, and intraluminal vesicle formation. Unlike ESCRT-I and ESCRT-II, which are stable protein complexes, ESCRT-III

[1] This work is supported by the U.S. National Science Foundation (grant no. IOS–0958066 and IOS–1456300) and the Natural Science Foundation of China (grant no. 2013C150203).

* Address correspondence to zhixiang@purdue.edu.

The author responsible for distribution of materials integral to the findings presented in this article in accordance with the policy described in the Instructions for Authors (www.plantphysiol.org) is: Zhixiang Chen (zhixiang@purdue.edu).

F.W. designed some of the experiments, performed most of the experiments, analyzed the data, and wrote part of the article; Y.Y., Z.W., and J.Z. performed some of the experiments; B.F. provided technical assistance and performed some of the experiments; Z.C. conceived the project, designed the experiments, analyzed the data, and wrote most of the article.

www.plantphysiol.org/cgi/doi/10.1104/pp.15.00518

proteins are monomers in the cytoplasm and only form complexes on the endosomal membrane. Disassembly of ESCRT-III, however, is not spontaneous but, rather, requires catalysis by the Vacuolar protein sorting 4p (Vps4p)/Suppressor of K^+ Transport Growth Defect1 (SKD1) AAA ATPase together with its positive regulator Vacuolar protein sorting20-associated1 (Vta1)/LIP5 in an ATP-dependent reaction (Babst et al., 1998; Fujita et al., 2004; Scott et al., 2005; Azmi et al., 2006; Lottridge et al., 2006). In yeast and mammalian cells, both Vps4p/SKD1 and Vta1/LIP5 are critical players of MVB biogenesis (Yeo et al., 2003; Shiflett et al., 2004; Ward et al., 2005; Azmi et al., 2006).

As sessile organisms, plants are constantly exposed to a wide range of biotic and abiotic stresses and, through evolution, have developed a battery of complicated adaptive mechanisms. Studies over the past decade have provided increasing evidence for the association of vesicle trafficking with plant responses to both biotic and abiotic stresses. Plant immune responses to biotic stresses consists of two interconnected branches: pattern-triggered immunity and effector-triggered immunity, which are conferred by pattern-recognition receptors and RESISTANCE (R) proteins, respectively. A number of pattern-recognition receptors, such as Arabidopsis (*Arabidopsis thaliana*) Flagellin-sensitive2 and R proteins, become associated with late endosomes/MVBs upon pattern and effector recognition, respectively, and there is strong evidence for a critical role of the association with vesicles in plant disease resistance (Choi et al., 2013; Spallek et al., 2013). In the penetration resistance of cereal plants against powdery mildew fungal pathogens, which is conferred by local cell wall appositions (papillae), electron and confocal microscopy detected trafficking molecules through late endosomes/MVBs for delivering defense-related materials to papillae, thereby executing a timely and localized defense response to invading pathogens (An et al., 2006a, 2006b; Meyer et al., 2009; Böhlenius et al., 2010; Nielsen et al., 2012). Similar relocalization of defense-related molecules, such as the PENTRATION RESISTANCE3 ATP-binding cassette transporter for cell surface defense in response to conserved pathogen elicitors, has also been observed in Arabidopsis (Underwood and Somerville, 2013). There is also evidence for a role of late endosomes/MVBs in plant abiotic stress responses (Jou et al., 2004, 2006; Ho et al., 2010; Xia et al., 2013). Generally speaking, however, while there is a large body of evidence for a critical role of general vesicle trafficking in plant stress responses, there has been only a limited number of studies that address specifically the roles and regulation of MVBs in plant responses to biotic and abiotic stresses. Studies on the role of MVBs in plant immune responses have been largely through microscopic analysis of the accumulation of the late endosomes in response to pathogen infection or elicitor treatment. Genetic analysis of the role of MVBs in plant stress responses has not been straightforward, because mutants for genes essential for MVB biogenesis are often lethal (Haas et al., 2007; Spitzer et al., 2009). While constitutive MVB biogenesis is known to be essential in many cellular processes, it remains to be determined whether there are specific pathogen/stress-responsive pathways for increased MVB biogenesis during plant stress responses.

In Arabidopsis, disruption of the *SKD1* gene is lethal, and expression of an ATPase-deficient mutant SKD1 causes alterations in the endosomal system and ultimately cell death (Haas et al., 2007). Arabidopsis LIP5 interacts strongly with SKD1 and increases in vitro the ATPase activity of SKD1 by 4- to 5-fold (Haas et al., 2007). However, disruption of *LIP5* in Arabidopsis causes no major phenotypic alterations under normal growth conditions, indicating that the basal level of the SKD1 ATPase activity without stimulation by LIP5 is sufficient for plant growth and development (Haas et al., 2007). Recently, we reported the identification of Arabidopsis LIP5 as an interacting protein and a substrate of the pathogen-responsive mitogen-activated protein kinases (MAPKs) MPK6/MPK3 (Wang et al., 2014). Functional analysis with *lip5* transfer DNA (T-DNA) insertion mutants indicates that LIP5 plays a critical role in pathogen-induced MVB trafficking and in basal resistance to *Pseudomonas syringae* strains (Wang et al., 2014). The critical role of LIP5 in the plant immune system is dependent on its ability to interact with SKD1. Further analysis reveals that LIP5 is expressed at low levels in healthy plants, but its protein levels can be substantially elevated through phosphorylation by the pathogen-responsive MPK cascade. Mutation of MPK phosphorylation sites in LIP5 does not affect its interaction with SKD1 but reduces its stability and, as a result, compromises its ability to complement the basal resistance of the *lip5* mutants. These results provide genetic evidence for a critical role of induced MVB biogenesis in plant basal resistance and establish an important mechanism for the regulation of vesicle trafficking during plant-pathogen interactions (Wang et al., 2014).

In this study, we report that the LIP5-regulated MVB pathway is also a critical cellular process during plant responses to abiotic stresses. Disruption of *LIP5* causes compromised tolerance to both heat and salt stresses. The critical role of LIP5 in plant tolerance to abiotic stresses is again dependent on its ability to interact with SKD1. When compared with wild-type plants, *lip5* mutants accumulate increased levels of ubiquitinated protein aggregates, suggesting a possible role of LIP5-regulated MVB trafficking as a critical route for the degradation of heat-damaged proteins. Compromised salt tolerance of the *lip5* mutants was associated with an increased accumulation of cellular NaCl but reduced levels of cellular reactive oxygen species (ROS), which have been implicated in the signaling of salt stress responses (Kaye et al., 2011; Xie et al., 2011). The roles of LIP5 and its phosphorylation by MPK3/6 in plant responses to heat and salt stresses were also investigated. These results collectively provide important insights into the role and regulation of pathogen- and stress-responsive MVB biogenesis in broad plant stress responses.

RESULTS

Arabidopsis *lip5* Mutants Were Hypersensitive to Heat and Salt Stresses

We recently reported a functional analysis of Arabidopsis LIP5 through the characterization of two independent T-DNA insertion mutants for the gene (Wang et al., 2014). The *lip5-1* and *lip5-2* null mutants each contains a T-DNA insertion in the last exon of *LIP5*, and both appear to be null based on quantitative real-time PCR. Although no major phenotypes were observed under normal growth conditions, both mutants were highly susceptible to the bacterial pathogen *P. syringae* (Wang et al., 2014). Thus, LIP5 plays an important role in plant immune responses to pathogens. To determine whether LIP5 plays a critical role in plant tolerance to abiotic stresses, we analyzed the responses of the *lip5* mutants to heat and salt stresses. To test heat tolerance, we placed 5-week-old wild-type and *lip5* plants in a 45°C growth chamber for 8 h followed by 3 to 5 d of recovery at room temperature. For heat-treated wild-type plants, only small areas of old leaves displayed symptoms of dehydration, but a majority of the leaves remained green and viable after the recovery (Fig. 1A). On the other hand, all of the leaves from the *lip5* mutant plants exhibited extensive wilting after 8 h at 45°C, and the plants were unable to recover after 3 to 5 d at room temperature (Fig. 1A). We also placed 3-week-old seedlings of wild-type and *lip5* plants in a 45°C growth chamber for 8 h and scored the survival rates after recovery for 5 d at room temperature. As shown in Figure 1, B and C, more than 85% of wild-type seedlings but only approximately 10% of *lip5* mutant seedlings survived after the heat stress. These observations indicated that the heat tolerance of the *lip5* mutants was substantially compromised.

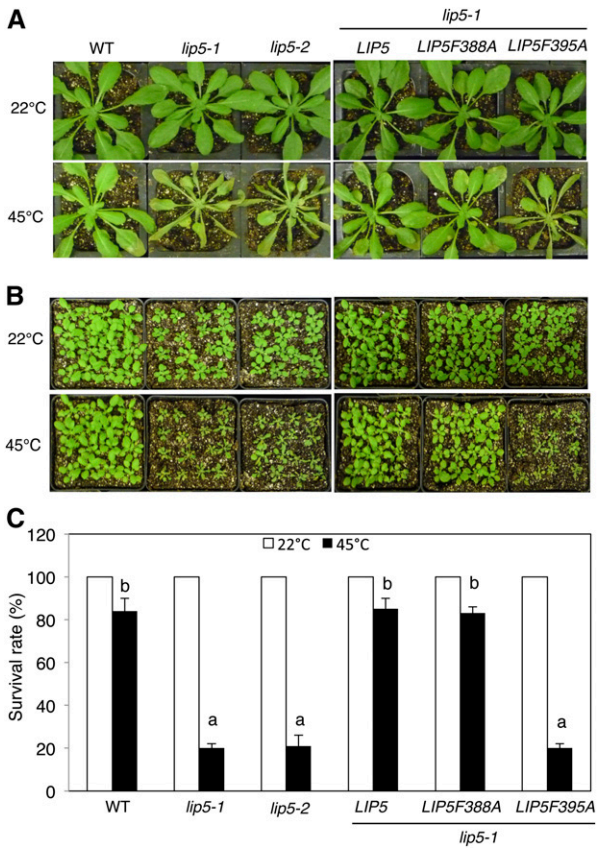

Figure 1. Hypersensitivity of the *lip5* mutants to heat stress. A, Representative images of 5-week-old Arabidopsis plants after 8 h at 45°C and 3 to 5 d of recovery at 22°C. B, Representative images of 3-week-old Arabidopsis plants after 8 h at 45°C and 3 to 5 d of recovery at 22°C. C, Survival rate of 3-week-old plants after 8 h at 45°C and 3 to 5 d of recovery at 22°C. Means and SE were calculated from three experiments. According to Duncan's multiple range test ($P = 0.05$), means do not differ significantly if they are indicated with the same letter. WT, Wild type.

We also tested the responses of the *lip5* mutants to salt stress by comparing wild-type and *lip5* seeds for germination and growth on one-half-strength Murashige and Skoog (MS) medium supplemented with 0 or 150 mM NaCl. At 0 mM NaCl, 100% of wild-type and *lip5* mutant seeds germinated to produce green and expanded cotyledons within 5 d (Fig. 2, A and B). At 150 mM NaCl, again, 100% of wild-type seeds produced green and expanded cotyledons but only approximately 10% of *lip5* mutant seeds produced green and expanded cotyledons at 5 d post germination (Fig. 2, A and B). In addition, we compared wild-type and *lip5* plants for root growth. At 0 mM NaCl, there was no significant difference in root length between the wild type and *lip5* mutants (Fig. 2, A and C). At 150 mM NaCl, the root growth of wild-type plants was reduced by approximately 50% when compared with the seedlings grown at 0 mM NaCl, but the *lip5* mutants showed approximately 80% reduction in root length when compared with the seedlings grown at 0 mM NaCl (Fig. 2, A and C). These results indicated that the *lip5* mutants were also compromised in salt tolerance.

The Role of LIP5 in Heat and Salt Tolerance Is Dependent on Interaction with SKD1

LIP5 is a positive regulator of SKD1 through physical interaction and stimulation of the ATPase activity of SKD1 (Haas et al., 2007). To determine whether the role of LIP5 in plant tolerance to heat and salt stresses is due to its action as a positive regulator of SKD1, we performed genetic complementation of the *lip5-1* mutant with *LIP5* genes. The C-terminal domain of yeast (*Saccharomyces cerevisiae*) LIP5 (Vta1) mediates LIP5 dimerization, and both subunits are required for the interaction with SKD1(VPS4) and for its function as a positive SKD1 regulator (Xiao et al., 2008). Analysis using site-directed mutagenesis further revealed that two conserved C-terminal domain residues of yeast LIP5 (Vta1), Tyr-303 and Tyr-310, were required for interacting with SKD1(VPS4) and stimulating its ATPase activity but dispensable for maintaining their dimeric structure (Xiao et al., 2008). In Arabidopsis LIP5, Phe-388 and Phe-395 are the corresponding residues for Tyr-303

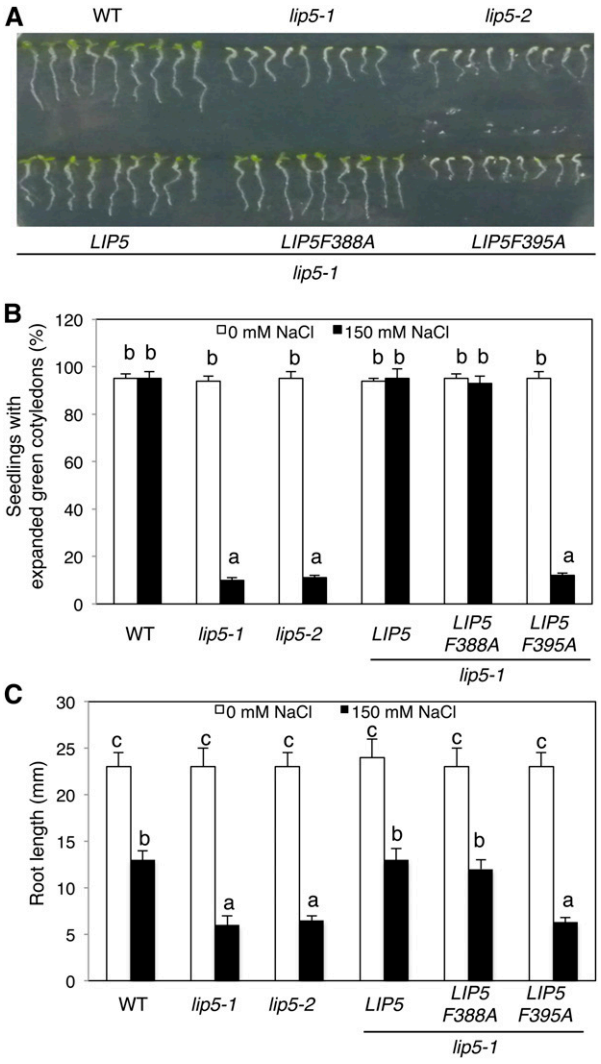

Figure 2. Hypersensitivity of the *lip5* mutants to salt stress. A, Arabidopsis seeds of the wild type (WT), *lip5-1* and *lip5-2* mutants, and transgenic lines were surface sterilized and sown on one-half-strength MS medium supplemented with 150 mM NaCl. Photographs were taken 2 d post stratification and 5 d post germination. B, Percentages of seedlings with green/expanded cotyledons determined at 5 d post germination. C, Root length of seedlings determined at 5 d post germination. Means and SE were calculated from three experiments. According to Duncan's multiple range test ($P = 0.05$), means do not differ significantly if they are indicated with the same letter.

and Tyr-310 of yeast LIP5 (Vta1), respectively. We generated mutant Arabidopsis LIP5 (F388A and F395A) in which either of the Phe residues was mutated into Ala residues. Yeast two-hybrid assays showed that, while wild-type LIP5 is a strong interactor of SKD1, LIP5F388A interacted weakly with SKD1, based on quantitative assays of the *Lactose Operon Gene Z* (*LacZ*) reporter gene expression (Wang et al., 2014). By contrast, no interaction of LIP5F395A with SKD1 was detected in yeast cells using the *LacZ* reporter gene assays (Wang et al., 2014).

To perform genetic complementation, we transformed myc-tagged wild-type and mutant *LIP5* genes under the control of the cauliflower mosaic virus (CaMV) *35S* promoter into the *lip5-1* mutant plants. Transformant lines were identified, and those expressing similar levels of the *LIP5* transgenes based on western blotting were compared for responses to heat and salt stresses. As expected, transformation of wild-type *LIP5* restored tolerance to heat and salt stresses of *lip5-1* (Figs. 1 and 2). In contrast, in the transgenic *lip5* mutant expressing mutant *LIP5F395A*, there was no restoration of heat or salt stress tolerance (Figs. 1 and 2). LIP5F388A, a weak SKD1 interactor, also complemented the *lip5* mutant for heat and salt stress tolerance (Figs. 1 and 2), most likely due to its overexpression driven by the strong CaMV *35S* promoter in the transgenic plants. These results indicated that interaction with SKD1 is necessary for the critical role of LIP5 in plant tolerance to heat and salt stresses.

Increased Accumulation of Ubiquitinated Aggregated Proteins in *lip5* Mutants under Heat Stress

Heat stress causes the accumulation of misfolded and damaged proteins, which are highly toxic, as they can bind inappropriately to important cellular components. To protect against potential proteotoxic stress, the cell relies on a complex protein quality control system, which consists of molecular chaperones such as Heat Shock Protein70 that promote the folding and refolding of nonnative proteins, and the protein degradation systems, which remove misfolded and damaged proteins. Most soluble misfolded proteins are degraded through the ubiquitin proteasome system (UPS). Misfolded and damaged proteins are prone to aggregate and may become difficult to unfold and pass through the narrow 20S proteasome core of UPS. These aggregated proteins can be targeted by selective autophagy for degradation. We have recently shown that CHIP, a chaperone-associated E3 ubiquitin ligase from Arabidopsis implicated in mediating the degradation of nonnative proteins by 26S proteasomes, acts additively with Neighbor of Breast Cancer1 Gene1 (NBR1)-mediated selective autophagy in protection against stress-induced proteotoxicity (Zhou et al., 2013, 2014). In the *chip* and *nbr1* single and double mutants, compromised heat tolerance is associated with increased accumulation of ubiquitinated protein aggregates under heat stress (Zhou et al., 2013, 2014).

To analyze whether the compromised heat tolerance of the *lip5* mutants was also associated with the increased accumulation of ubiquitinated proteins, we placed wild-type and *lip5-1* mutant plants in a 45°C growth chamber and collected leaves after 0, 4, and 8 h of heat stress. Total proteins were isolated from heat-stressed leaves using a detergent-containing extraction buffer, and ubiquitinated proteins were detected by western blotting using an anti-ubiquitin antibody after separation by SDS-PAGE. As shown in Figure 3A, the

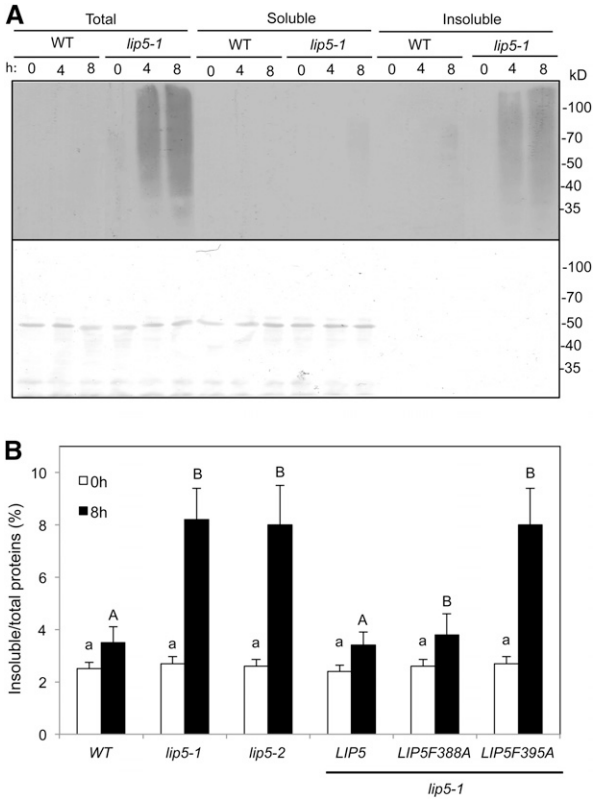

Figure 3. Increased accumulation of ubiquitinated aggregated proteins in the *lip5* mutants under heat stress. A, Five-week-old wild-type (WT) and *lip5-1* Arabidopsis plants were placed in a 45°C chamber, and leaf samples were collected at the indicated hours. Total proteins (Total) were extracted and separated into soluble and insoluble fractions by low-speed centrifugation. Soluble proteins in the supernatant (Soluble) and insoluble proteins in the pellets (Insoluble) isolated from equal amounts of total proteins for each sample were separated on SDS-PAGE gels, and ubiquitinated proteins were detected using western blotting with an anti-ubiquitin monoclonal antibody (top). Ponceau staining of the membrane blot before antibody probing is also shown (bottom). B, Accumulation of insoluble proteins. Leaf tissues from the wild type, *lip5* mutants, and transgenic lines were collected at the indicated hours under 45°C for the preparation of total, soluble, and insoluble proteins. Total proteins in the starting homogenates and insoluble proteins in the last pellets were determined to calculate the percentages of insoluble proteins. According to Duncan's multiple range test ($P = 0.05$), means do not differ significantly if they are indicated with the same letter.

levels of ubiquitinated proteins were very low, and there was little induction by heat stress in either wild-type or mutant plants. The levels of ubiquitinated proteins in the *lip5-1* mutant plants were also very low prior to heat stress (Fig. 3A). After 4 and 8 h of heat stress under 45°C, the levels of ubiquitinated proteins in the *lip5* mutants were elevated at much higher levels than in wild-type plants (Fig. 3A). To determine whether heat-induced ubiquitinated proteins were soluble proteins or detergent-resistant insoluble protein aggregates, we fractionated the total proteins into soluble and insoluble fractions using low-speed centrifugation. Soluble and detergent-resistant protein aggregates isolated from equal amounts of total proteins for each genotype/treatment were also separated by SDS-PAGE and subjected to immunoblot analysis for the detection of ubiquitinated proteins using an anti-ubiquitin antibody. As shown in Figure 3A, very low levels of ubiquitinated proteins were detected in the soluble fraction even from heat-treated *lip5* mutant plants. By contrast, high levels of ubiquitinated proteins were detected in the insoluble fraction from heat-treated *lip5* mutant plants, even though insoluble proteins accounted for only a few percentages of total proteins loaded on the gel (Fig. 3A). These results indicate that a majority of ubiquitinated proteins in heat-treated *lip5* mutant plants are insoluble protein aggregates. Furthermore, we found increased accumulation of detergent-resistant protein aggregates in heat-treated *lip5-1* and *lip5-2* mutant plants (Fig. 3B), as has been observed previously with heat-sensitive *nbr1* and *chip* mutants (Zhou et al., 2013, 2014). Complementation of the *lip5-1* mutant with the *LIP5* or *LIP5F388A* gene not only restored heat tolerance but also reduced the heat-induced accumulation of insoluble protein aggregates (Figs. 1 and 3B). By contrast, expression of LIP5F395A mutant protein, which is unable to interact with SKD1, failed to restore heat tolerance or decrease the accumulation of insoluble protein aggregates under heat stress (Figs. 1 and 3B). These results indicated that LIP5's role in plant heat tolerance is associated with the production and/or processing of heat-induced protein aggregates, and this role of LIP5 is also dependent on its interaction with SKD1.

Increased Accumulation of NaCl in *lip5* Mutants under Salt Stress

The ability to limit sodium accumulation in cytoplasm plays a critical role in salt tolerance (Jiang et al., 2010). To determine whether the increased sensitivity of *lip5* mutants to NaCl is associated with increased accumulation of the salt, we analyzed intracellular free sodium using SodiumGreen diacetate, a cell-permeable sodium indicator that is not fluorescent in the apoplast but becomes fluorescent upon entering cells and binding the sodium ions. SodiumGreen imaging was performed on 5-d-old Arabidopsis seedlings after 0 and 16 h of exposure to 150 mM NaCl in liquid one-half-strength MS medium. As shown in Figure 4, sodium accumulated in the root cells of wild-type plants after 16 h of NaCl treatment, as indicated by increased SodiumGreen fluorescence when compared with that of untreated seedlings. In *lip5* mutants, the basal sodium levels in their root cells were similar to those in wild-type seedlings (Fig. 4). After NaCl treatment, however, the *lip5* mutants accumulated approximately 30% more sodium than wild-type roots (Fig. 4). In addition, SodiumGreen signals were detected in both cytosol and vacuoles in salt-treated wild-type and *lip5* root cells, but in a majority of cells, the signals were generally stronger in the cytosol than in the vacuoles (Fig. 4A).

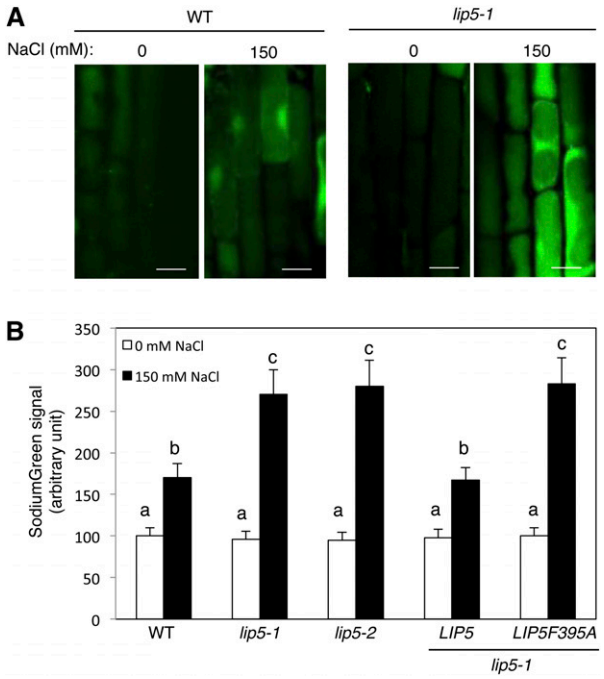

Figure 4. Increased accumulation of sodium ions in the *lip5* mutants. Five-day-old seedlings were treated with 0 or 150 mM NaCl for 20 h. Intracellular free sodium levels were analyzed using SodiumGreen staining. A, Representative confocal images of SodiumGreen staining. Bars = 100 μm. B, Quantified total SodiumGreen fluorescent signal intensity. Fluorescent signal intensity was determined from 20 Z stack images of root epidermal cells. Means and SE were calculated from images of 10 independent roots (20 images per root). According to Duncan's multiple range test ($P = 0.05$), means do not differ significantly if they are indicated with the same letter. WT, Wild type.

To examine whether the critical role of LIP5 in limiting the accumulation of intracellular sodium ions is dependent on its interaction with SKD1, we again compared the *lip5* mutant plants expressing either wild-type *LIP5* or the *LIP5F395A* mutant gene. Complementation of the *lip5* mutant by the wild-type *LIP5* gene driven by the CaMV *35S* promoter resulted in both increased salt tolerance and decreased accumulation of intracellular sodium ions (Figs. 2 and 4). By contrast, expression of *LIP5F395A* failed to restore salt tolerance or limit the accumulation of sodium ions in root cells under salt stress (Figs. 2 and 4). These results indicated that LIP5's role in plant salt tolerance and limiting the accumulation of sodium ions in the cytoplasm of root cells is dependent on its interaction with SKD1.

Increased Root Swelling of *lip5* Mutants under Salt Stress

It has been shown previously that, in Arabidopsis root tip cells, hydroponic treatment with a high concentration of NaCl (200 mM) leads to a decrease in the number of small acidic Na^+-containing vesicles and a rapid increase in the vacuolar volume (Hamaji et al., 2009). The increased vacuolar volume resulting from increased vesicle trafficking and fusion, however, was not associated with increased cell volume, which could help increase the cytoplasmic osmotic potential (Hamaji et al., 2009). However, we found that the cells immediately above the root tips swelled after NaCl treatment, and the swelling was greater in *lip5* mutants than in wild-type plants. As shown in Figure 5, root swelling started at 12 h after NaCl treatment, with the appearance in some roots of small but detectable bulges at approximately 0.5 mm above the root tips. In the wild type, the swelling became more apparent when the duration of salt stress increased to 16 and 22 h, but they were largely limited to the same region immediately above the root tips (Fig. 5). In the *lip5* mutants, NaCl-induced swelling was significantly more severe, as indicated by the earlier appearance and larger sizes of the bulges than those from wild-type plants (Fig. 5). In addition, the bulges in the *lip5* mutant roots expanded upward with prolonged salt stress, and by 22 h of NaCl treatment, the edges of the swelling bulges already reached approximately 1 mm above the root tips (Fig. 5). Some swollen root hair-like structures were also observed in both the wild type and *lip5* mutants at 22 h but not at earlier time points after NaCl treatment (Fig. 5A).

Compromised ROS Production under Salt Stress in the *lip5* Mutants

Increased production of ROS is observed in plant cells under biotic and abiotic stresses, including salt

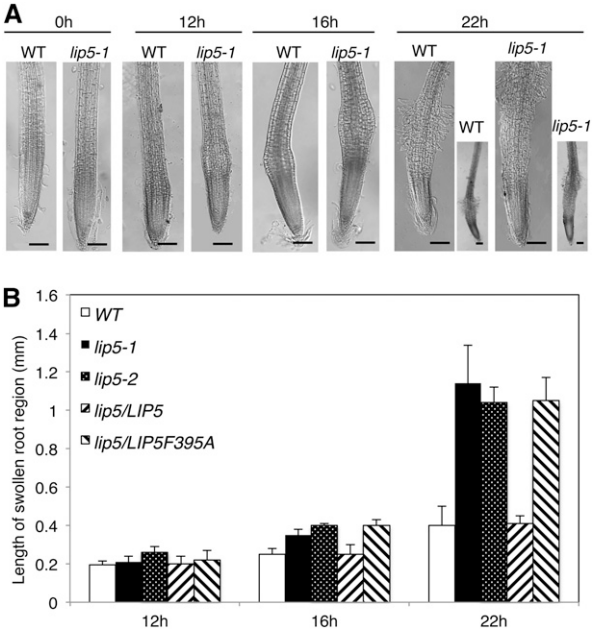

Figure 5. Increased root swelling of the *lip5* mutants under prolonged salt stress. Five-day-old seedlings were treated with 150 mM NaCl for the indicated amounts of time. A, Representative images of wild-type (WT) and *lip5-1* roots after salt stress. Bars = 100 μm. B, Lengths of swollen regions from the wild type, *lip5-1*, *lip5-2*, and transgenic lines. The lengths of the swollen region were defined by the longitudinal length of the smallest rectangles that encompass the swollen region. Means and SE of swollen root length were calculated from more than 10 roots.

stress. Excessively high levels of ROS can damage proteins and lipids and, thus, compromise stress tolerance (Gill and Tuteja, 2010). ROS at low levels, however, function as signaling molecules during plant stress responses through the regulation of transporter activity (Chung et al., 2008), transcriptional reprogramming (Foyer and Noctor, 2005), and the inhibition of root-to-shoot sodium transport (Jiang et al., 2012). To determine the role of LIP5 in salt-induced ROS production, we compared wild-type and *lip5* mutant plants for the NaCl-induced accumulation of ROS using the fluorescent dye 2′,7′-dichlorodihydrofluorescein diacetate (H_2DCFDA), a well-known ROS detector that is not fluorescent when chemically reduced but becomes fluorescent after cellular oxidation and the removal of acetate groups by cellular esterases (Hempel et al., 1999; Rastogi et al., 2010). The levels of ROS indicated by the H_2DCFDA fluorescence intensities were very low in both wild-type and *lip5* mutant plants in the absence of NaCl stress (Fig. 6). After treatment with 150 mM NaCl, the H_2DCFDA fluorescence intensities increased substantially in the wild type but only weakly in the *lip5* mutant roots (Fig. 6). Thus, salt-induced ROS production was compromised in the *lip5* mutant plants. Complementation of the *lip5-1* mutant with the wild-type *LIP5* but not the *LIP5F395A* gene restored salt-induced ROS production (Fig. 6B), indicating that interaction with SKD1 is again necessary for the positive role of LIP5 in salt-induced ROS production. Despite the difference between the wild type and the *lip5* mutant in salt-induced ROS accumulation, we observed no significant difference in transcript levels for a number of genes encoding proteins involved in the scavenging or production of ROS (Supplemental Fig. S1). These genes include three for catalases (*CAT1*, *CAT2*, and *CAT3*), three for copper superoxide dismutases (*SOD1*, *SOD2*, and *SOD3*), and *RbohD* and *RbohF* encoding the two most abundant NADPH oxidases (Supplemental Fig. S1).

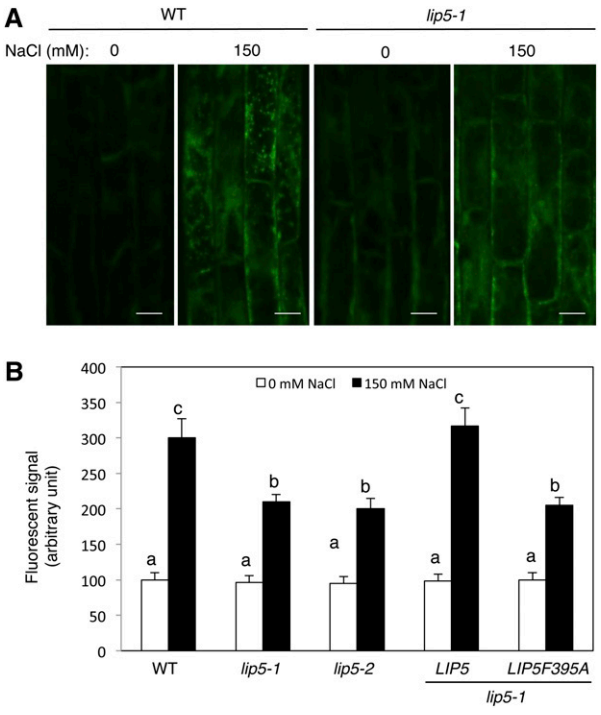

Figure 6. Compromised ROS production under salt stress in the *lip5* mutants. Five-day-old seedlings were treated with 0 or 150 mM NaCl for 20 h. ROS levels were analyzed using H_2DCFDA staining. A, Representative confocal images of Arabidopsis root epidermal cells of the wild type (WT) and the *lip5-1* mutant after H_2DCFDA staining. Bars = 100 μm. B, Signal intensity of H_2DCFDA in stained Arabidopsis root epidermal cells of the wild type, *lip5-1*, *lip5-2*, and transgenic lines. Means and SE were calculated from images of 10 independent roots (more than 20 images per root). According to Duncan's multiple range test ($P = 0.05$), means do not differ significantly if they are indicated with the same letter.

Compromised Phenotype of *lip5* in Stress-Induced Vesicle Trafficking

We recently showed that the critical role of LIP5 in plant basal resistance is through its regulatory role in pathogen-induced cellular vesicle trafficking (Wang et al., 2014). Using the styryl dye FM1-43 as a fluorescent endocytosis marker, the Arabidopsis Rab GTPase6 (Ara6)-GFP MVB marker, and transmission electron microscopy, we demonstrated that pathogen infection increases the formation of both intracellular MVBs and exosome-like paramural vesicles situated between the plasma membrane and the cell wall in a largely LIP5-dependent manner (Wang et al., 2014). To examine whether the reduced heat and salt tolerance of the *lip5* mutants was also associated with compromised vesicle trafficking under stress conditions, we first compared wild-type and *lip5* mutant plants for heat- or salt-induced endocytosis using FM1-43. The membrane-selective FM1-43, which fluoresces significantly only in a lipid-rich membrane, can enter the cells by endocytic vesicles derived from the plasma membrane (Emans et al., 2002; Bolte et al., 2004). For determining heat-induced endocytic activities, however, we found the results using FM1-43 to be unreproducible, most likely because dramatic temperature shifting may affect a number of membrane properties. For determining salt-induced endocytic activities, we analyzed internalized FM1-43 signal after 20 min of incubation with the dye in Arabidopsis roots with or without prior NaCl treatment. Without prior salt stress (at 0 mM NaCl), we observed similar levels of internalized FM1-43 signal in wild-type and *lip5* roots (Fig. 7). With prior NaCl treatment, the intensity of internalized FM1-43 signal increased by almost 3-fold in wild-type roots (Fig. 7). Unlike in wild-type plants, however, there was only a 30% increase in internalized FM1-43 fluorescence by NaCl treatment in the *lip5* roots (Fig. 7). These results indicate that salt stress stimulates endocytosis and vesicle trafficking in plant cells in a largely LIP5-dependent manner. Complementation of the *lip5-1* mutant with the wild-type *LIP5*

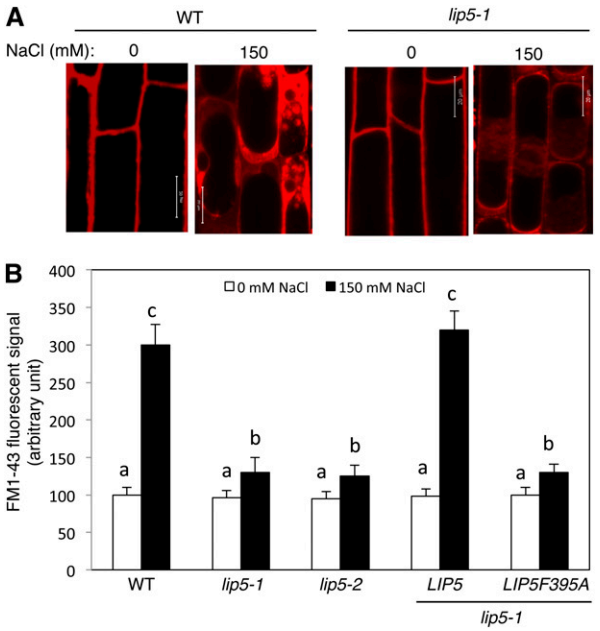

Figure 7. Compromised endocytosis in the *lip5* mutants under salt stress. Five-day-old seedlings were treated with 0 or 150 mM NaCl for 20 h. Salt-induced endocytosis was analyzed using FM1-43. A, Representative confocal images of Arabidopsis root epidermal cells of the wild type (WT) and the *lip5-1* mutant after FM1-43 staining. Bars = 100 μm. B, Signal intensity of internalized FM1-43 in Arabidopsis root epidermal cells of the wild type, *lip5-1*, *lip5-2*, and transgenic lines. The fluorescent signal intensity of internalized FM1-43 was determined from 20 Z stack images of root epidermal cells. Means and SE were calculated from images of 10 independent roots (20 images per root). According to Duncan's multiple range test ($P = 0.05$), means do not differ significantly if they are indicated with the same letter.

but not the *LIP5F395A* gene restored salt-induced vesicle trafficking (Fig. 7B).

To further analyze the role of LIP5 in stress-induced MVB formation, we used previously generated transgenic wild-type and *lip5-1* mutant plants expressing a GFP-fused MVB marker protein, the ARA6/Rat sarcoma (Ras)-like protein in brain F1 (RabF1) GTPase (Haas et al., 2007; Wang et al., 2014). The transgenic plants were placed in a 25°C or 45°C growth chamber for 2 h, and their leaf cells were observed for the ARA6-GFP signals. At 25°C, we detected similar levels of punctate ARA6-GFP signals in wild-type and *lip5* mutant plants (Fig. 8A). After heat stress at 45°C, the numbers of punctate ARA6-GFP signals were increased by approximately 35% in wild-type plants but were little changed in the *lip5* mutant plants (Fig. 8A). These results indicated that heat stress induced MVB biogenesis in plant cells in a LIP5-dependent manner. For examining NaCl-induced MVB formation, the transgenic plant seedlings expressing the MVB marker were placed on MS medium containing 0 or 150 mM NaCl. At 0 mM NaCl, we again detected similar levels of punctate ARA6-GFP signals in the roots of wild-type and *lip5* mutant seedlings. At 150 mM NaCl, the numbers of punctate ARA6-GFP signals were increased by approximately 60% in wild-type plants but were little changed in the *lip5* mutant plants (Fig. 8B). Similar results showing a LIP5-dependent increase in MVB biogenesis after NaCl treatment were also obtained with another GFP-fused MVB marker protein, the ARA7 GTPase (Ueda et al., 2001; Supplemental Fig. S2).

Subcellular Localization of LIP5 under Heat and Salt Stresses

To examine the subcellular localization of LIP5 under heat and salt stresses, we used a previously generated transgenic wild-type line expressing a *LIP5-GFP* fusion gene. In untreated control Arabidopsis plants expressing *LIP5-GFP*, both dispersed and punctate fluorescent signals were observed predominantly in the cytoplasm of leaf epidermal cells (Fig. 9A). The number of fluorescent punctate signals in the cells was more than doubled after heat shock treatment (Fig. 9A). Similarly, salt treatment resulted in more than an 80% increase in the number of the punctate LIP5-GFP fluorescent signals in root cells of the transgenic plants (Fig. 9B). Thus, both heat and salt stresses increased the relocalization of LIP5 from the cytosol to an endosomal compartment. It was recently shown that pathogen infection also increased the number of punctate LIP5-GFP fluorescent signals, which were largely colabeled by the ARA6-red fluorescent protein MVB marker (Wang et al., 2014). To

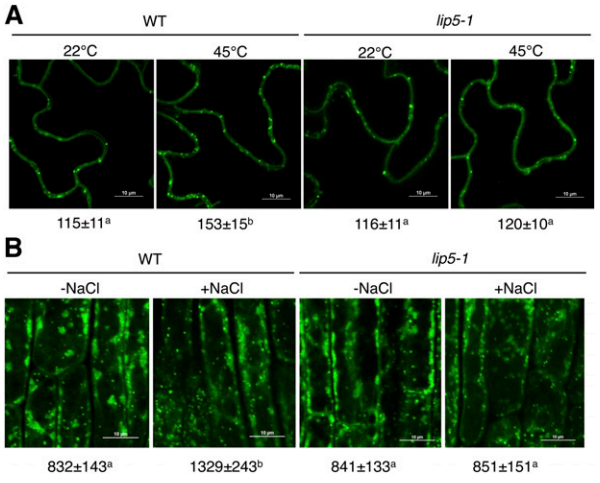

Figure 8. Induced formation of ARA6-GFP-labeled MVBs under salt and heat stress in a LIP5-dependent manner. A, Representative confocal images and statistical analysis of ARA6-GFP-labeled MVBs in leaves of the wild type (WT) and *lip5-1* before or after heat stress. Bars = 10 μm. B, Representative confocal images and statistical analysis of ARA6-GFP-labeled MVBs of root epidermal cells of the wild type and *lip5-1* before or after salt stress. Bars = 10 μm. The numbers of fluorescent endosomal structures per microscopic field (100 × 100 μm) are indicated below the images. Means and SE were calculated from three experiments. According to Duncan's multiple range test ($P = 0.05$), means do not differ significantly if they are indicated with the same letter.

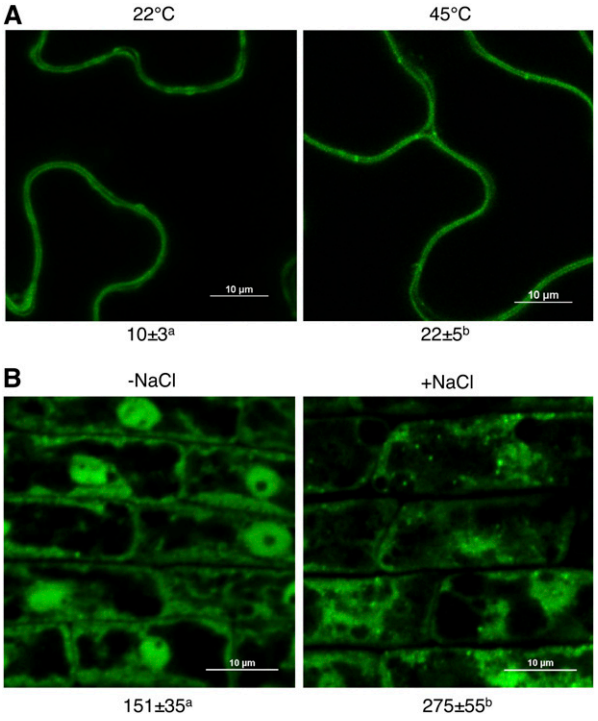

Figure 9. LIP5-GFP-labeled punctate signals were induced by salt and heat stress. A, Representative confocal images and statistical analysis of leaves of LIP5-GFP transgenic plants before or after heat stress. Bars = 10 μm. B, Representative confocal images and statistical analysis of root epidermal cells of LIP5-GFP transgenic plants before or after salt stress. Bars = 10 μm. The numbers of internalized fluorescent endosomal structures per microscopic field (100 × 100 μm) are indicated below the images. Means and SE were calculated from three experiments. According to Duncan's multiple range test (P = 0.05), means do not differ significantly if they are indicated with the same letter.

determine whether the increased number of LIP5-GFP vesicles reflects the relocalization of LIP5 from the cytosol to the MVBs, we analyzed the change of LIP5 levels in the microsomal membrane upon heat stress. For this purpose, we used a transgenic line stably expressing myc-tagged LIP5 under the control of the constitutive CaMV 35S promoter. Both total and microsomal proteins were isolated from the transgenic LIP5 line before and after heat stress, and the levels of myc-tagged LIP5 were detected by immunoblot analysis using an anti-myc antibody. As shown in Supplemental Figure S3, heat stress did not affect the total LIP5 protein levels but significantly increased the level of LIP5 in the microsomal fraction. These results support that biotic and abiotic stresses trigger the increased association of LIP5 with MVBs.

In Vivo Phosphorylation of LIP5 under Salt and Heat Stresses

Arabidopsis LIP5 interacts with pathogen/stress-responsive MPK3/MPK6 and is phosphorylated in vitro by activated MPK3 and MPK6 and in vivo upon the expression of MPK3/6-activating NtMEK2^{DD} and pathogen infection (Wang et al., 2014). Mutation of MPK phosphorylation sites in LIP5 does not affect the interaction with SKD1 but reduces the stability of the mutant LIP5 (Wang et al., 2014). To determine the possible in vivo phosphorylation and stability enhancement of LIP5 under abiotic stresses, we used previously generated transgenic plants expressing similar levels of transcripts for a myc-tagged wild-type LIP5 (LIP5^{WT}) or a mutant LIP5 protein in which all six potential MAPK phosphorylation Ser or Thr residues were mutated into Ala (LIP5^{6A}; Fig. 10A). These transgenic plants were placed in a 45°C growth chamber, and total proteins were isolated from these transgenic plants at different time points and analyzed by western blotting using anti-myc antibody after separation on an SDS-PAGE gel. As reported previously, even with

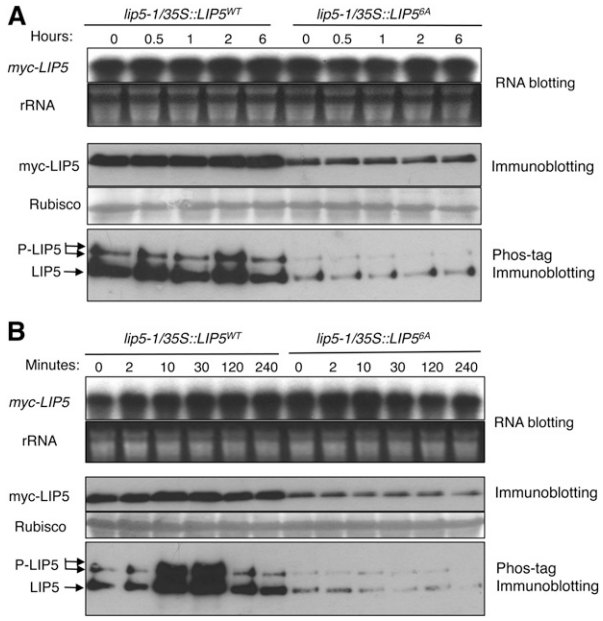

Figure 10. In vivo phosphorylation of LIP5 under abiotic stresses. A, In vivo phosphorylation of LIP5 under heat stress. Transgenic *lip5-1/35S::LIP5*^{WT} and *lip5-1/35S::LIP5*^{6A} plants with similar levels of *myc-LIP5* transcripts were treated in a 45°C chamber, and leaf samples were collected at the indicated time points. The levels of *myc-LIP5* transcripts were analyzed by RNA blotting using a ^{32}P-labeled myc tag DNA fragment as probe (top). Ethidium bromide staining of ribosomal RNA (rRNA) is shown for the assessment of equal loading. Total proteins were also isolated and separated on a regular SDS-PAGE (middle) gel and a Phos-tag SDS-PAGE (bottom) gel. The myc-LIP5^{WT} and myc-LIP5^{6A} proteins were detected with an anti-myc monoclonal antibody. Rubisco staining of the regular SDS-PAGE gel was used to assess equal protein loading. B, In vivo phosphorylation of LIP5 in salt stress. Seedlings of transgenic *lip5-1/myc-LIP5*^{WT} and *lip5-1/myc-LIP5*^{6A} lines containing similar levels of *myc-LIP5* transcripts were treated with 150 mM NaCl. Samples were collected at the indicated hours for total RNA and protein isolation. RNA blotting, regular immunoblotting, and Phos-tag immunoblotting were performed as in A.

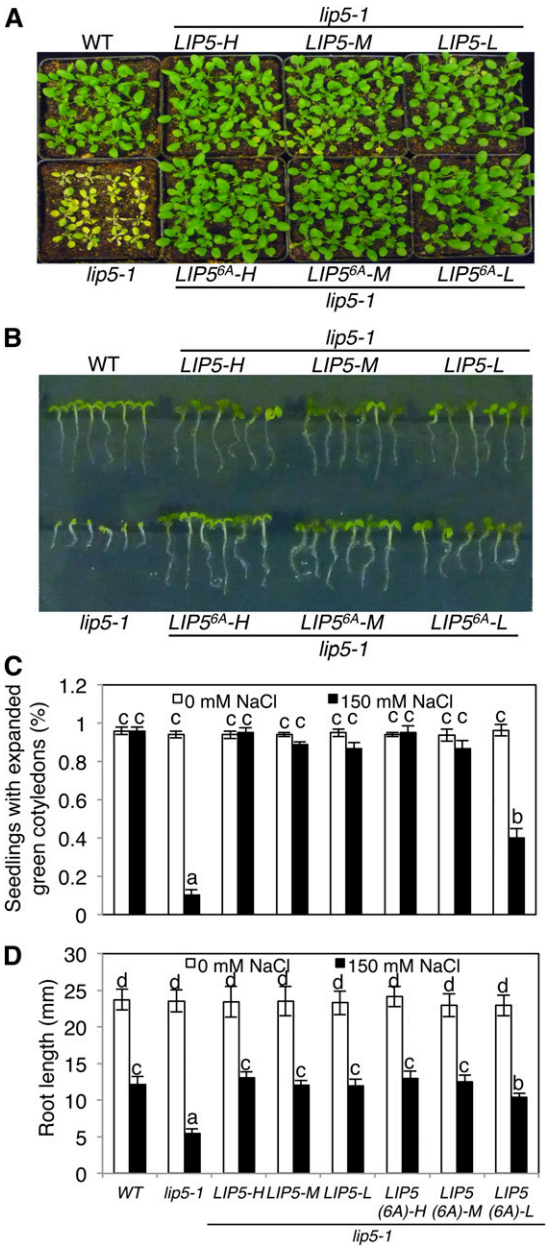

Figure 11. Role of phosphorylation-regulated LIP5 stability in plant abiotic stress tolerance. A, Phosphorylation-regulated LIP5 stability and heat tolerance. Three-week-old plants of the wild type (WT), *lip5-1*, and *lip5-1/myc-LIP5^{WT}* and *lip5-1/myc-LIP5^{6A}* lines with similarly high (H), medium (M), and low (L) levels of *myc-LIP5* transcripts were treated for 8 h in a 45°C chamber and then recovered at room temperature in a growth room for 3 to 5 d before photography. B, Phosphorylation-regulated LIP5 stability and salt tolerance. Arabidopsis seeds of the wild type, *lip5-1*, and *lip5-1/myc-LIP5^{WT}* and *lip5-1/myc-LIP5^{6A}* lines with similarly high, medium, and low levels of *myc-LIP5* transcripts were surface sterilized and sown on one-half-strength MS medium supplemented with 150 mM NaCl. Photographs were taken 2 d post stratification and 5 d post germination. C and D, Percentages of seedlings with green/expanded cotyledons (C) and root length of seedlings (D) were determined at 5 d post germination. Means and SE were calculated from three experiments. According to Duncan's multiple range test ($P = 0.05$), means do not differ significantly if they are indicated with the same letter.

similar transcript levels, the protein levels of myc-LIP5^{WT} were higher than those of myc-LIP5^{6A} even before heat stress (Fig. 10A). After heat stress, the protein levels of both myc-LIP5^{WT} and myc-LIP5^{6A} remained unchanged (Fig. 10A). Thus, the protein stability of LIP5 is positively regulated by the basal activity of MAPKs but was not further enhanced by heat stress.

The isolated total proteins were also examined for in vivo phosphorylation of LIP5 using the Phos-tag mobility shift assay. Before heat treatment, we detected two major bands of LIP5^{WT}, representing the unphosphorylated and phosphorylated LIP5 (Fig. 10A). We also detected two relatively weak bands for LIP5^{6A}, as reported previously, likely because of other sites in LIP5 besides the six Pro-directed Ser and Thr residues that are subjected to phosphorylation by unknown kinases. After heat stress, the intensities of both unphosphorylated and phosphorylated bands even for LIP5^{WT} remained largely unchanged (Fig. 10A). Thus, before heat stress, the basal levels of LIP5^{WT} were higher than those of LIP5^{6A}, because the stability of LIP5^{WT} was enhanced due to phosphorylation by the basal levels of MAPKs. However, the stability of LIP5^{WT} was not further increased by heat stress, likely because there was no further increase in LIP5 phosphorylation by MAPKs under heat stress.

We also analyzed the in vivo phosphorylation and stability of LIP5 under salt stress. Again, the extent of phosphorylation and the protein levels of myc-LIP5^{WT} were higher than those of myc-LIP5^{6A} before salt stress (Fig. 10B). Shortly after salt stress (at both 10 and 30 min), however, we observed a further increase in phosphorylation of myc-LIP5^{WT}, as indicated by increased intensities of retarded LIP5 bands on the Phos-tag gel (Fig. 10B). This increase in the phosphorylation of LIP5 was associated with significantly elevated levels of myc-LIP5^{WT} proteins, as indicated from western blotting of both the regular and Phos-tag gels (Fig. 10B). By contrast, no increase in either phosphorylation or protein levels of myc-LIP5^{6A} was observed after salt stress (Fig. 10B). Thus, the protein stability of LIP5 is positively regulated by the basal activities of MAPKs and is further enhanced by salt stress.

To further determine the role of MPK3/MPK6 in the regulation of LIP5 stability, we also examined the stability of LIP5 in an *mpk3 mpk6* double mutant expressing an MPK6 protein with the large gatekeeping amino acid, Tyr-144, changed to Gly (*mpk3mpk6/P$_{mpk6}$:MPK6^{YG}*; Xu et al., 2014). The ATP analog 4-amino-1-tert-butyl-3-(1′-naphthyl)pyrazolo[3,4-d]pyrimidine (NA-PP1), due to its bulkier side chain, can specifically inhibit MPK6^{YG} but not wild-type kinases (Xu et al., 2014). In the absence of NA-PP1, functional MPK6^{YG} can rescue the embryo lethality of the *mpk3 mpk6* double mutant (Xu et al., 2014). We transformed myc-tagged *LIP5* into the *mpk3mpk6/P$_{mpk6}$:MPK6^{YG}* conditional mutant. Leaves from the transgenic plants were treated with the protein synthesis inhibitor cycloheximide (CHX), NA-PP1, or both, and total proteins were then isolated, separated on a Phos-tag gel, and detected with

an anti-myc antibody for LIP5 phosphorylation and protein levels (Supplemental Fig. S4). Treatment with CHX for 90 min resulted in a significant reduction in LIP5 protein levels, which were recovered if the treatment was increased to 180 min (Supplemental Fig. S4). Treatment of NA-PP1 reduced both phosphorylation and protein levels of LIP5 after both 90 and 180 min of treatment (Supplemental Fig. S4). Interestingly, treatment of both CHX and NA-PP1 for 90 min resulted in a drastic reduction in the LIP5 protein level, and this reduction apparently did not result from lethal toxicity, because increasing the time of treatment to 180 min actually led to a significant recovery of LIP5 proteins (Supplemental Fig. S3). These results strongly suggest that there is a rapid turnover of LIP5 proteins in the absence of functional MPK3 and MPK6.

Role of Phosphorylation-Regulated LIP5 Stability in Plant Abiotic Stress Tolerance

To determine the importance of LIP5 phosphorylation by the stress-responsive MPKs, we compared the ability of myc-LIP5^{WT} and myc-LIP5^{6A} in complementing the *lip5* mutant phenotype. As described previously (Wang et al., 2014), we initially used the native *LIP5* promoter to drive the *myc-LIP5* transgenes, but even the *LIP5* promoter-driven *myc-LIP5^{WT}* construct (*P$_{LIP5}$::myc-LIP5^{WT}*) failed to complement the *lip5* mutant phenotype, and there was no detectable *LIP5* transcript or myc-LIP5^{WT} protein in the *lip5-1/P$_{LIP5}$::myc-LIP5^{WT}* lines. Thus, additional noncoding sequences other than the promoter are necessary for sufficient levels of *LIP5* expression. For this reason, we used the CaMV *35S*-driven *LIP5* (*35S::LIP5^{WT}* and *35S::LIP5^{6A}*) constructs and obtained three types of transgenic lines for each construct that contained high (H), medium (M), or low (L) levels of the *myc-LIP5* transgene (Wang et al., 2014). Protein immunoblotting using an anti-myc antibody revealed that there were similarly high levels of myc-LIP5 proteins in the transgenic *lip5-1/35S::LIP5^{WT}-H* and *lip5-1/35S::LIP5^{6A}-H* lines, which contained relatively high levels of *myc-LIP5* transcripts (Wang et al., 2014). On the other hand, when comparing the transgenic lines that contained medium levels of *myc-LIP5* transcripts, we observed that the protein levels of myc-LIP5^{WT} in the *lip5-1/35S::LIP5^{WT}-M* lines were substantially higher than those of myc-LIP5^{6A} in the *lip5-1/35S::LIP5^{6A}-M* lines (Wang et al., 2014). When comparing the transgenic lines that contained low levels of *myc-LIP5* transcripts, we again observed that the protein levels of myc-LIP5^{WT} in the *lip5-1/35S::LIP5^{WT}-L* lines were substantially higher than those of myc-LIP5^{6A} in the *lip5-1/35S::LIP5^{6A}-L* lines (Wang et al., 2014). Significantly, in *lip5* mutants containing high, medium, or low levels of either LIP5^{WT} or LIP5^{6A}, the heat tolerance was equally restored to wild-type levels (Fig. 11A). Thus, while LIP5 is required for plant heat tolerance, its enhanced stability by phosphorylation is not necessary for its full ability to complement the compromised heat sensitivity of the *lip5* mutant plants.

We used the same transgenic *lip5* lines expressing three different levels of LIP5^{WT} or LIP5^{6A} to determine the role of LIP5 phosphorylation in salt tolerance. As shown in Figure 11, B to D, when the *lip5* transgenic lines expressing high, medium, and low levels of myc-LIP5^{WT} were examined on growth medium containing 150 mM NaCl, the tolerance was fully restored to wild-type levels based on both germination rates and root growth. Likewise, when the *lip5* transgenic lines expressing high and medium levels of myc-LIP5^{6A} were examined on growth medium containing 150 mM NaCl, the tolerance was also fully restored to the levels of wild-type plants (Fig. 11, B–D). However, when the *lip5* transgenic lines expressing low levels of myc-LIP5^{6A} were examined on NaCl-containing growth medium, the tolerance was only partially restored to the levels of wild-type plants (Fig. 11, B–D). These results indicated that enhanced LIP5 stability by phosphorylation is necessary for its full ability to complement the compromised salt sensitivity of the *lip5* mutant plants.

DISCUSSION

Arabidopsis LIP5 interacts strongly with SKD1 and stimulates the ATPase activity of SKD1 by 4- to 5-fold (Haas et al., 2007). However, the *lip5* knockout mutants in Arabidopsis are largely normal in growth and development under normal growth conditions, indicating that the basal levels of the SKD1 ATPase activity are sufficient for constitutive MVB biogenesis for plant growth and development (Haas et al., 2007). This is consistent with the observations that the basal levels of FM1-43-labeled endocytic vesicles and ARA6-GFP- or ARA7-GFP-labeled MVBs were not significantly reduced in the *lip5* mutants when compared with those of wild-type plants under normal growth conditions (Wang et al., 2014; Figs. 7 and 8; Supplemental Fig. S2). On the other hand, the *lip5* mutants are hypersusceptible to the bacterial pathogen *P. syringae*, and this compromised disease resistance is associated with defects in pathogen-induced formation of both intracellular MVBs and exosome-like paramural vesicles situated between the plasma membrane and the cell wall (Wang et al., 2014). In this study, we demonstrated that *lip5* mutants were also hypersensitive to heat and salt stress, and the critical role of LIP5 in plant tolerance to the abiotic stresses is dependent on its ability to interact with SKD1 (Figs. 1 and 2). Furthermore, the hypersensitivity of the *lip5* mutants to heat and salt stress is associated with defects in heat- and salt-induced, but not the constitutive formation of, endocytic vesicles and intracellular MVBs (Figs. 7 and 8). Therefore, our comprehensive functional analysis of LIP5 provides strong evidence for a critical role of pathogen/stress-responsive MVB biogenesis in broad plant stress responses.

Heat stress causes proteotoxic stress due to the production of misfolded/denatured proteins that can bind inappropriately to important cellular components.

There is now a mounting body of evidence that efficient removal of these misfolded/damaged proteins, particularly under stress conditions, is critical for the survival of cells. In eukaryotic cells, two protein degradation systems, the UPS and autophagy, are major pathways for the degradation of misfolded and damaged proteins (Arias and Cuervo, 2011; Amm et al., 2014). The UPS is involved in the degradation of nonnative cytoplasmic proteins from various intracellular compartments, while autophagy can target large protein aggregates and damaged organelles during stress responses. Direct comparison revealed that the Arabidopsis *lip5* mutants were even more heat sensitive than the Arabidopsis *chip nbr1* double mutants (F. Wang and Z. Chen, unpublished data). Furthermore, as observed in the *chip* and *nbr1* mutants (Zhou et al., 2014), the increased heat sensitivity of *lip5* mutant plants was associated with an increased accumulation of heat-induced protein aggregates (Fig. 3). As a major degradation route in the endocytic pathway, LIP5-regulated MVB trafficking may protect plant cells against heat-induced proteotoxicity through the degradation of heat-damaged membrane proteins in the vacuole. Upon synthesis in the endoplasmic reticulum (ER), misfolded nonnative membrane proteins are subject to degradation by the UPS. This involves retrotranslocation of the misfolded membrane proteins from the ER to the cytoplasm, where they are progressively cleaved by 26S proteasomes. However, those heat-damaged nonnative membrane proteins in post-ER compartments are subjected to peripheral quality control along the late secretory and endocytic pathways as well as at the plasma membrane (Okiyoneda et al., 2010). Those membrane proteins in the cis-Golgi compartment that escape the ER with limited conformational defects can be retrieved back into the ER or targeted from the trans-Golgi network and other post-ER compartments, including the plasma membrane, by vesicular transport for degradation in the lysosome or vacuole (Okiyoneda et al., 2010). Studies in mammalian systems have shown that ubiquitination also acts as a signal for the degradation of nonnative membrane proteins by the peripheral quality control machinery (Okiyoneda et al., 2010). ESCRT-dependent concentration and inward budding of ubiquitinated membrane protein cargo from the limiting membrane of endosomes during heat-induced MVB formation would provide a solution for the topological problem of the degradation of polytopic membrane proteins. In mammalian cells, a number of recent studies have linked the chaperone-dependent CHIP E3 ubiquitin ligase to the endocytic trafficking and lysosomal degradation of a number of plasma membrane proteins (Okiyoneda et al., 2011). As both CHIP and LIP5 are evolutionarily highly conserved, it would be of interest to examine possible functional interactions between the two proteins in protection against proteotoxic stresses in plant cells.

A great deal is already known about the complex molecular basis of plant responses to salt stresses from the extensive characterization of regulatory proteins involved in signaling processes and the protein transporters involved in ion transport. Dynamic vesicle trafficking has also emerged as a critical cellular process in the regulation of plant responses to salt stress (Hamaji et al., 2009). One potential role of vesicle trafficking in plant salt tolerance is to facilitate vacuolar compartmentalization of the internalized cation to reduce its toxic effect in the cytosol. When Arabidopsis seedlings were treated with high levels of NaCl, their root tip cells displayed rapid changes in vacuolar volume, decreases in the number of small acid compartments, and the accumulation of Na^+ in the central vacuole (Hamaji et al., 2009). Overexpression of an intracellular vesicle-trafficking protein, AtRab7(AtRabG3e), resulted in increased salt tolerance associated with an increased uptake and preferential accumulation of NaCl in vacuoles (Mazel et al., 2004). Through comparative analysis of the wild type and *lip5* mutants, we provided genetic evidence for a critical role of salt-induced MVB trafficking in plant salt stress responses. However, the increased sensitivity of the *lip5* mutants to NaCl was associated with an increased Na^+ accumulation in the roots (Fig. 4). Thus, in addition to a role in vacuolar compartmentalization of the internalized Na^+, MVB trafficking may be involved in other processes that limit overall cellular Na^+ accumulation under salt stress, either through reducing Na^+ influx or facilitating Na^+ efflux. For example, stress-induced, LIP5-regulated MVB trafficking may down-regulate the protein levels of those Na^+ transporters important for Na^+ entry into plant roots through increased endocytosis and subsequent degradation in vacuoles. In addition, MVBs in plant cells can fuse not only with vacuoles but also with the plasma membrane, and the MVB fusion with the plasma membrane may play a critical role not only in plant focal defense against invading pathogens, most likely through the release of antimicrobial compounds (An et al., 2006a, 2006b; Meyer et al., 2009; Böhlenius et al., 2010; Nielsen et al., 2012), but also in plant responses to abiotic stresses such as salt. Recent studies on Arabidopsis Rab5 GTPases also supported an important role of the MVB-plasma membrane fusion in salt tolerance (Ebine et al., 2011, 2012). Arabidopsis contains three Rab5 GTPases, ARA6/RAB5C/RABF1, ARA7/RAB5B/RABF2B, and Rab5 Homolog A1/RAB5A/RABF2A. ARA6 was structurally distinct and controlled MVB fusion with the plasma membrane, while ARA7 and RHA1 redundantly controlled the MVB-vacuole fusion. Mutation of ARA6 impaired normal salt stress tolerance, and overexpression of constitutively active $ARA6^{QL}$ improved salt stress performance. $ARA6^{QL}$-GFP formed speckles at the plasma membrane subdomains during salt stress, suggesting ARA6-dependent active and specific transport of unknown cargoes under salt stressed conditions (Ebine et al., 2011, 2012). Membrane proteins such as Salt Overly Sensitive1 and other ion transporters could be targeted by salt-induced endocytosis and recycled to membranes with altered activity or location through the fusion of

ARA6-labeled MVBs with the plasma membrane (Ebine et al., 2011, 2012).

Other possible cargoes for salt-induced MVB trafficking could include ROS-producing NADPH oxidases. A number of studies have shown that NADPH oxidase-dependent ROS was induced by salt stress in Arabidopsis seedling roots and functioned as a positive regulator of salt tolerance by signaling salt stress responses. Mutations of genes involved in phosphatidylinositol signaling, which regulates vesicle trafficking, not only compromised salt tolerance but also the salt-induced intracellular production of ROS by NADPH oxidases (Kaye et al., 2011). Although NADPH oxidases normally reside in the plasma membrane, they can also be targeted by endocytosis and assembled into active forms in the internal membranes, and endosomal ROS production plays critical roles in a number of biological processes, including preinflammatory immune responses (Rubinek and Levy, 1993; Casbon et al., 2009). In Arabidopsis, salt-induced ROS is inhibited by an NADPH oxidase inhibitor and diminished in the NADPH oxidase mutants (Kaye et al., 2011). In addition, the production of ROS detected with H_2DCFDA revealed a speckled intracellular distribution, which overlapped with FM1-64 fluorescent signals (Kaye et al., 2011). These observations suggest the endosomal production of ROS by activated NADPH oxidases under salt stress. Likewise, the compromised salt tolerance of the *lip5* mutant plants was also associated with reduced levels of intracellular ROS in *lip5* root cells (Fig. 6). The strong phenotype of the *lip5* mutants in the salt-induced production of intracellular ROS supports a regulatory role of stress-induced MVBs in plant stress responses.

We previously showed that the stability of LIP5 is enhanced through phosphorylation by pathogen-responsive MPK3/6 and that the resulting increase in LIP5 protein levels is important for pathogen-induced vesicle trafficking and plant basal resistance (Wang et al., 2014). Using the same transgenic lines expressing myc-tagged $LIP5^{WT}$ and $LIP5^{6A}$, we demonstrated increased phosphorylation of LIP5 under salt stress, which was accompanied by increased stability and, consequently, elevated protein levels of LIP5 (Fig. 10B). Complementation of *lip5* mutant plants by wild-type and phosphorylation mutant *LIP5* genes further revealed a critical role of the salt-induced, phosphorylation-mediated increase in LIP5 stability in plant salt tolerance (Fig. 11, B–D). Intriguingly, although there was a significant basal level of LIP5 phosphorylation, which increases the basal level of LIP5, there was no further increase in LIP5 protein phosphorylation or protein stability under heat stress (Fig. 10A). By contrast, a recent study reports that heat stress activates MPK6, which specifically targets the major heat stress transcription factor Heat Shock Transcription Factor A2 by phosphorylating it on Thr-249 and changes its intracellular localization (Evrard et al., 2013). Phosphorylation of other heat stress transcription factors, such as HsfA4, involved in responses to salt and oxidative stresses by stress-responsive MPK3/6 has also been reported (Pérez-Salamó et al., 2014). Apparently, LIP5 is a poor substrate of MPK3/6 under heat stress when compared with the highly inducible and probably more abundant Hsf proteins. In addition, while the *lip5* mutants are highly sensitive to heat stress, this mutant phenotype of the *lip5* mutants could be fully rescued by the $LIP5^{6A}$ mutant gene even at a low expression level (Fig. 11A). It appears that while LIP5 is required for plant heat tolerance, its basal level without further stabilization by MPK3/6-catalyzed phosphorylation is sufficient for heat-induced MVB biogenesis. Therefore, while LIP5-regulated MVB trafficking plays a critical role in plant responses to a broad spectrum of biotic and abiotic stresses, its regulation has apparently diversified and been tailored to specific stress responses.

MATERIALS AND METHODS

Plant Genotypes and Growth Conditions

Arabidopsis (*Arabidopsis thaliana*) plants were grown in growth chambers at 22°C and 120 E m^{-2} light on a photoperiod of 12 h of light and 12 h of dark. All Arabidopsis materials were in the Columbia-0 background. Mutant and transgenic lines for *LIP5* and other genes have been described previously (Wang et al., 2014).

Heat and Salt Stress Treatments

The heat tolerance of mature plants or seedlings was analyzed as described previously (Zhou et al., 2013). For testing salt tolerance, the seeds were directly germinated on one-half-strength MS medium supplemented with 0 or 150 mM NaCl. Five days after germination, seedlings with or without green/expanded cotyledons were counted and root lengths were measured.

Analysis of Insoluble/Ubiquitinated Proteins

The preparation and analysis of soluble and insoluble proteins from heat-stressed plant leaves were performed as described previously (Zhou et al., 2013). Briefly, leaf samples were ground in liquid nitrogen and homogenized in an extraction buffer (50 mM Tris, pH 8, 150 mM NaCl, 1 mM EDTA, 0.1% [v/v] Triton X-100, 1 mM phenylmethylsulfonyl fluoride, and 0.1% [v/v] 2-mercaptoethanol). Total extracts were filtered through 300- and 100-μm nylon mesh, and volumes were measured. Total protein concentrations were determined by the Bio-Rad protein assay kit using bovine serum albumin as a standard, and total proteins were separated into the soluble and insoluble fractions by centrifugation at 2,200*g* for 10 min at 4°C. The insoluble pellet fractions were washed three times with extraction buffer. The concentrations of proteins in the homogenates (total proteins), the first supernatants (soluble proteins), and the last pellets (insoluble proteins) were determined using the Bio-Rad protein assay kit. Soluble and insoluble proteins isolated from the amounts of total proteins for each sample were adjusted to the same volumes and separated on an SDS polyacrylamide gel. After transfer to a nitrocellular membrane, ubiquitinated proteins were detected by western blotting using anti-ubiquitin monoclonal antibody.

Fluorescence Microscopy

Confocal imaging of ARA6-GFP, ARA7-GFP, and LIP5-GFP fluorescent signals was performed as described previously (Wang et al., 2014). Fluorescence microscopy of FM1-43 (Life Technologies) internalization in Arabidopsis roots was also performed as described previously (Wang et al., 2014), with minor changes of the concentration of FM1-43 and staining time reduced to 10 μM and 20 min, respectively. Concentrations and staining times were 20 μM and 20 min for H_2DCFDA (Life Technologies) and 20 μM and 60 min for SodiumGreen (Life Technologies), respectively. The wavelength settings of confocal microscopy were as follows: excitation at 488 nm and emission at 600 to 650 nm for FM1-43, excitation at 488 nm and emission at 550 to 600 nm for H_2DCFDA, and excitation at 488 nm and emission at 550 to 600 nm for SodiumGreen. For the quantification of signal intensity, Z stack images of

stained root tissue were captured starting from the surface of the root. Two neighboring areas that represent the greatest number of epidermal cells, yet including no cortex cells or any other cell types, were averaged into one image. The signal intensity was calculated as the total signal of that image divided by the area of the epidermal cell section within the image. Ten independent roots were quantified and statistically analyzed for each genotype/treatment.

RNA Isolation and Quantitative Real-Time PCR

Isolation of total RNA and quantitative real-time PCR were performed as described previously (Zhou et al., 2013). Gene-specific reverse transcription-PCR primers were designed based on their complementary DNA sequences (Supplemental Table S1). The Arabidopsis *ACTIN2* gene was used as an internal control as described previously (Zhou et al., 2013).

Immunoblot Analysis of Microsomal Membrane-Associated LIP5 Proteins

Plants from a homozygous transgenic line constitutively expressing the myc-tagged LIP5 at a relatively low level were heat treated at 45°C for 4 h. Total and microsomal proteins were isolated from leaf tissues harvested before and after heat stress as described previously (Abas and Luschnig, 2010) and separated by SDS-PAGE. The myc-LIP5 proteins were detected by immunoblotting using an anti-myc antibody.

In Vivo Phosphorylation of LIP5

Assays of the in vivo phosphorylation of LIP5 were performed as described previously (Wang et al., 2014). Total proteins and microsomal proteins were isolated from leaf tissues harvested before and after heat stress as described previously.

Assays of LIP5 Proteins in the *mpk3mpk6/P$_{mpk6}$:MPK6^{YG}* Conditional Mutant

The *35S:myc-LIP5* construct was transformed into the *mpk3mpk6/P$_{mpk6}$:MPK6^{YG}* conditional mutant. Leaves of transgenic plants expressing a modest level of myc-tagged LIP5 were treated with CHX (600 μM), NA-PP1 (10 μM), or both. Leaf samples were collected at 0, 90, and 180 min for protein extraction. Protein separation and myc-LIP5 protein detection by immunoblotting were performed as described previously (Wang et al., 2014).

Sequence data from this article can be found in the GenBank/EMBL data libraries under accession numbers LIP5 (At4g26750), SKD1 (At2g27600), MPK3 (At3g45640), MPK6 (At2g43790), Ara6 (At3g54840), and Ara7 (At4g19640).

Supplemental Data

The following supplemental materials are available.

Supplemental Figure S1. Expression of genes involved in ROS production and scavenging under salt stress.

Supplemental Figure S2. Induced formation of ARA7-GFP labeled endosome signals under salt stress in an LIP5-dependent manner.

Supplemental Figure S3. Increased association of myc-LIP5 with microsomal membrane under heat stress.

Supplemental Figure S4. LIP5 proteins in the *mpk3 mpk6* double mutant.

Supplemental Table S1. Primers for quantitative real-time PCR.

ACKNOWLEDGMENTS

We thank Dr. Marisa Otegui (University of Wisconsin) for the *lip5-1* mutant and the *ARA6* and *ARA7* constructs, the Arabidopsis Biological Resource Center at Ohio State University and the Nottingham Arabidopsis Stock Centre for other Arabidopsis mutants, and Dr. Shuqun Zhang (University of Missouri) for the *mpk3mpk6/P$_{mpk6}$:MPK6^{YG}* conditional mutant.

Received April 8, 2015; accepted July 30, 2015; published July 30, 2015.

LITERATURE CITED

Abas L, Luschnig C (2010) Maximum yields of microsomal-type membranes from small amounts of plant material without requiring ultracentrifugation. Anal Biochem **401:** 217–227

Amm I, Sommer T, Wolf DH (2014) Protein quality control and elimination of protein waste: the role of the ubiquitin-proteasome system. Biochim Biophys Acta **1843:** 182–196

An Q, Ehlers K, Kogel KH, van Bel AJ, Hückelhoven R (2006a) Multivesicular compartments proliferate in susceptible and resistant MLA12-barley leaves in response to infection by the biotrophic powdery mildew fungus. New Phytol **172:** 563–576

An Q, Hückelhoven R, Kogel KH, van Bel AJ (2006b) Multivesicular bodies participate in a cell wall-associated defence response in barley leaves attacked by the pathogenic powdery mildew fungus. Cell Microbiol **8:** 1009–1019

Arias E, Cuervo AM (2011) Chaperone-mediated autophagy in protein quality control. Curr Opin Cell Biol **23:** 184–189

Azmi I, Davies B, Dimaano C, Payne J, Eckert D, Babst M, Katzmann DJ (2006) Recycling of ESCRTs by the AAA-ATPase Vps4 is regulated by a conserved VSL region in Vta1. J Cell Biol **172:** 705–717

Babst M, Wendland B, Estepa EJ, Emr SD (1998) The Vps4p AAA ATPase regulates membrane association of a Vps protein complex required for normal endosome function. EMBO J **17:** 2982–2993

Böhlenius H, Mørch SM, Godfrey D, Nielsen ME, Thordal-Christensen H (2010) The multivesicular body-localized GTPase ARFA1b/1c is important for callose deposition and ROR2 syntaxin-dependent preinvasive basal defense in barley. Plant Cell **22:** 3831–3844

Bolte S, Talbot C, Boutte Y, Catrice O, Read ND, Satiat-Jeunemaitre B (2004) FM-dyes as experimental probes for dissecting vesicle trafficking in living plant cells. J Microsc **214:** 159–173

Casbon AJ, Allen LA, Dunn KW, Dinauer MC (2009) Macrophage NADPH oxidase flavocytochrome B localizes to the plasma membrane and Rab11-positive recycling endosomes. J Immunol **182:** 2325–2339

Choi SW, Tamaki T, Ebine K, Uemura T, Ueda T, Nakano A (2013) RABA members act in distinct steps of subcellular trafficking of the FLAGELLIN SENSING2 receptor. Plant Cell **25:** 1174–1187

Chung JS, Zhu JK, Bressan RA, Hasegawa PM, Shi H (2008) Reactive oxygen species mediate Na^+-induced SOS1 mRNA stability in Arabidopsis. Plant J **53:** 554–565

Contento AL, Bassham DC (2012) Structure and function of endosomes in plant cells. J Cell Sci **125:** 3511–3518

Ebine K, Fujimoto M, Okatani Y, Nishiyama T, Goh T, Ito E, Dainobu T, Nishitani A, Uemura T, Sato MH, et al (2011) A membrane trafficking pathway regulated by the plant-specific RAB GTPase ARA6. Nat Cell Biol **13:** 853–859

Ebine K, Miyakawa N, Fujimoto M, Uemura T, Nakano A, Ueda T (2012) Endosomal trafficking pathway regulated by ARA6, a RAB5 GTPase unique to plants. Small GTPases **3:** 23–27

Emans N, Zimmermann S, Fischer R (2002) Uptake of a fluorescent marker in plant cells is sensitive to brefeldin A and wortmannin. Plant Cell **14:** 71–86

Evrard A, Kumar M, Lecourieux D, Lucks J, von Koskull-Döring P, Hirt H (2013) Regulation of the heat stress response in Arabidopsis by MPK6-targeted phosphorylation of the heat stress factor HsfA2. PeerJ **1:** e59

Foyer CH, Noctor G (2005) Redox homeostasis and antioxidant signaling: a metabolic interface between stress perception and physiological responses. Plant Cell **17:** 1866–1875

Fujita H, Umezuki Y, Imamura K, Ishikawa D, Uchimura S, Nara A, Yoshimori T, Hayashizaki Y, Kawai J, Ishidoh K, et al (2004) Mammalian class E Vps proteins, SBP1 and mVps2/CHMP2A, interact with and regulate the function of an AAA-ATPase SKD1/Vps4B. J Cell Sci **117:** 2997–3009

Gill SS, Tuteja N (2010) Reactive oxygen species and antioxidant machinery in abiotic stress tolerance in crop plants. Plant Physiol Biochem **48:** 909–930

Haas TJ, Sliwinski MK, Martínez DE, Preuss M, Ebine K, Ueda T, Nielsen E, Odorizzi G, Otegui MS (2007) The *Arabidopsis* AAA ATPase

SKD1 is involved in multivesicular endosome function and interacts with its positive regulator LYST-INTERACTING PROTEIN5. Plant Cell **19:** 1295–1312

Hamaji K, Nagira M, Yoshida K, Ohnishi M, Oda Y, Uemura T, Goh T, Sato MH, Morita MT, Tasaka M, et al (2009) Dynamic aspects of ion accumulation by vesicle traffic under salt stress in Arabidopsis. Plant Cell Physiol **50:** 2023–2033

Hempel SL, Buettner GR, O'Malley YQ, Wessels DA, Flaherty DM (1999) Dihydrofluorescein diacetate is superior for detecting intracellular oxidants: comparison with 2′,7′-dichlorodihydrofluorescein diacetate, 5 (and 6)-carboxy-2′,7′-dichlorodihydrofluorescein diacetate, and dihydrorhodamine 123. Free Radic Biol Med **27:** 146–159

Ho LW, Yang TT, Shieh SS, Edwards GE, Yen HE (2010) Reduced expression of a vesicle trafficking-related ATPase SKD1 decreases salt tolerance in Arabidopsis. Funct Plant Biol **37:** 962–973

Jiang C, Belfield EJ, Mithani A, Visscher A, Ragoussis J, Mott R, Smith JA, Harberd NP (2012) ROS-mediated vascular homeostatic control of root-to-shoot soil Na delivery in Arabidopsis. EMBO J **31:** 4359–4370

Jiang X, Leidi EO, Pardo JM (2010) How do vacuolar NHX exchangers function in plant salt tolerance? Plant Signal Behav **5:** 792–795

Jou Y, Chiang CP, Jauh GY, Yen HE (2006) Functional characterization of ice plant SKD1, an AAA-type ATPase associated with the endoplasmic reticulum-Golgi network, and its role in adaptation to salt stress. Plant Physiol **141:** 135–146

Jou Y, Chou PH, He M, Hung Y, Yen HE (2004) Tissue-specific expression and functional complementation of a yeast potassium-uptake mutant by a salt-induced ice plant gene mcSKD1. Plant Mol Biol **54:** 881–893

Kaye Y, Golani Y, Singer Y, Leshem Y, Cohen G, Ercetin M, Gillaspy G, Levine A (2011) Inositol polyphosphate 5-phosphatase7 regulates the production of reactive oxygen species and salt tolerance in Arabidopsis. Plant Physiol **157:** 229–241

Lottridge JM, Flannery AR, Vincelli JL, Stevens TH (2006) Vta1p and Vps46p regulate the membrane association and ATPase activity of Vps4p at the yeast multivesicular body. Proc Natl Acad Sci USA **103:** 6202–6207

Mazel A, Leshem Y, Tiwari BS, Levine A (2004) Induction of salt and osmotic stress tolerance by overexpression of an intracellular vesicle trafficking protein AtRab7 (AtRabG3e). Plant Physiol **134:** 118–128

Meyer D, Pajonk S, Micali C, O'Connell R, Schulze-Lefert P (2009) Extracellular transport and integration of plant secretory proteins into pathogen-induced cell wall compartments. Plant J **57:** 986–999

Nielsen ME, Feechan A, Böhlenius H, Ueda T, Thordal-Christensen H (2012) Arabidopsis ARF-GTP exchange factor, GNOM, mediates transport required for innate immunity and focal accumulation of syntaxin PEN1. Proc Natl Acad Sci USA **109:** 11443–11448

Okiyoneda T, Apaja PM, Lukacs GL (2011) Protein quality control at the plasma membrane. Curr Opin Cell Biol **23:** 483–491

Okiyoneda T, Barrière H, Bagdány M, Rabeh WM, Du K, Höhfeld J, Young JC, Lukacs GL (2010) Peripheral protein quality control removes unfolded CFTR from the plasma membrane. Science **329:** 805–810

Pérez-Salamó I, Papdi C, Rigó G, Zsigmond L, Vilela B, Lumbreras V, Nagy I, Horváth B, Domoki M, Darula Z, et al (2014) The heat shock factor A4A confers salt tolerance and is regulated by oxidative stress and the mitogen-activated protein kinases MPK3 and MPK6. Plant Physiol **165:** 319–334

Rastogi RP, Singh SP, Häder DP, Sinha RP (2010) Detection of reactive oxygen species (ROS) by the oxidant-sensing probe 2′,7′-dichlorodihydrofluorescein diacetate in the cyanobacterium Anabaena variabilis PCC 7937. Biochem Biophys Res Commun **397:** 603–607

Reyes FC, Buono R, Otegui MS (2011) Plant endosomal trafficking pathways. Curr Opin Plant Biol **14:** 666–673

Rubinek T, Levy R (1993) Arachidonic acid increases the activity of the assembled NADPH oxidase in cytoplasmic membranes and endosomes. Biochim Biophys Acta **1176:** 51–58

Scott A, Chung HY, Gonciarz-Swiatek M, Hill GC, Whitby FG, Gaspar J, Holton JM, Viswanathan R, Ghaffarian S, Hill CP, et al (2005) Structural and mechanistic studies of VPS4 proteins. EMBO J **24:** 3658–3669

Shiflett SL, Ward DM, Huynh D, Vaughn MB, Simmons JC, Kaplan J (2004) Characterization of Vta1p, a class E Vps protein in Saccharomyces cerevisiae. J Biol Chem **279:** 10982–10990

Spallek T, Beck M, Ben Khaled S, Salomon S, Bourdais G, Schellmann S, Robatzek S (2013) ESCRT-I mediates FLS2 endosomal sorting and plant immunity. PLoS Genet **9:** e1004035

Spitzer C, Reyes FC, Buono R, Sliwinski MK, Haas TJ, Otegui MS (2009) The ESCRT-related CHMP1A and B proteins mediate multivesicular body sorting of auxin carriers in *Arabidopsis* and are required for plant development. Plant Cell **21:** 749–766

Ueda T, Yamaguchi M, Uchimiya H, Nakano A (2001) Ara6, a plant-unique novel type Rab GTPase, functions in the endocytic pathway of Arabidopsis thaliana. EMBO J **20:** 4730–4741

Underwood W, Somerville SC (2013) Perception of conserved pathogen elicitors at the plasma membrane leads to relocalization of the Arabidopsis PEN3 transporter. Proc Natl Acad Sci USA **110:** 12492–12497

Wang F, Shang Y, Fan B, Yu JQ, Chen Z (2014) Arabidopsis LIP5, a positive regulator of multivesicular body biogenesis, is a critical target of pathogen-responsive MAPK cascade in plant basal defense. PLoS Pathog **10:** e1004243

Ward DM, Vaughn MB, Shiflett SL, White PL, Pollock AL, Hill J, Schnegelberger R, Sundquist WI, Kaplan J (2005) The role of LIP5 and CHMP5 in multivesicular body formation and HIV-1 budding in mammalian cells. J Biol Chem **280:** 10548–10555

Winter V, Hauser MT (2006) Exploring the ESCRTing machinery in eukaryotes. Trends Plant Sci **11:** 115–123

Xia Z, Wei Y, Sun K, Wu J, Wang Y, Wu K (2013) The maize AAA-type protein SKD1 confers enhanced salt and drought stress tolerance in transgenic tobacco by interacting with Lyst-interacting protein 5. PLoS ONE **8:** e69787

Xiao J, Xia H, Zhou J, Azmi IF, Davies BA, Katzmann DJ, Xu Z (2008) Structural basis of Vta1 function in the multivesicular body sorting pathway. Dev Cell **14:** 37–49

Xie YJ, Xu S, Han B, Wu MZ, Yuan XX, Han Y, Gu Q, Xu DK, Yang Q, Shen WB (2011) Evidence of Arabidopsis salt acclimation induced by up-regulation of HY1 and the regulatory role of RbohD-derived reactive oxygen species synthesis. Plant J **66:** 280–292

Xu J, Xie J, Yan C, Zou X, Ren D, Zhang S (2014) A chemical genetic approach demonstrates that MPK3/MPK6 activation and NADPH oxidase-mediated oxidative burst are two independent signaling events in plant immunity. Plant J **77:** 222–234

Yeo SC, Xu L, Ren J, Boulton VJ, Wagle MD, Liu C, Ren G, Wong P, Zahn R, Sasajala P, et al (2003) Vps20p and Vta1p interact with Vps4p and function in multivesicular body sorting and endosomal transport in Saccharomyces cerevisiae. J Cell Sci **116:** 3957–3970

Zhou J, Wang J, Cheng Y, Chi YJ, Fan B, Yu JQ, Chen Z (2013) NBR1-mediated selective autophagy targets insoluble ubiquitinated protein aggregates in plant stress responses. PLoS Genet **9:** e1003196

Zhou J, Zhang Y, Qi J, Chi Y, Fan B, Yu JQ, Chen Z (2014) E3 ubiquitin ligase CHIP and NBR1-mediated selective autophagy protect additively against proteotoxicity in plant stress responses. PLoS Genet **10:** e1004116